Microelectronics Reliability 88–90 (2018) 855–858

Contents lists available at ScienceDirect

Microelectronics Reliability

journal homepage: www.elsevier.com/locate/microrel

Degradation mechanisms of heterogeneous III-V/Silicon loop-mirror laser diodes for photonic integrated circuits

M. Buffolo[a,*], M. Pietrobon[a], C. De Santi[a,b], F. Samparisi[a], M.L. Davenport[c], J.E. Bowers[c], G. Meneghesso[a], E. Zanoni[a], M. Meneghini[a]

[a] Department of Information Engineering, University of Padova, Padova, Italy
[b] Centro Giorgio Levi Cases, University of Padova, Via Marzolo 9, 35131 Padova, Italy
[c] Department of Electrical and Computing Engineering, University of Santa Barbara, California, USA

ARTICLE INFO

Keywords:
Reliability
Degradation
Laser-diode
Silicon-photonics

ABSTRACT

This paper reports on the degradation processes of heterogeneous III-V/Silicon loop-mirrors laser-diodes designed as the optical sources for next-generation Photonic Integrated Circuits (PICs) operating at 1.55 μm. By submitting the devices to a series of constant-current accelerated aging experiments we were able to identify a common set of degradation mechanisms, including: (i) an increase in threshold current, (ii) a decrease of the sub-threshold emission, (iii) a decrease in the operating voltage of the device and (iv) a small decrease in the slope-efficiency of the laser. The strong correlation between these degradation processes suggests that the loss in optical performance experienced by the devices can be attributed to a decrease in the non-radiative carrier lifetime, as a consequence of the generation/propagation of defects towards the active region of the laser diodes.

1. Introduction

The integration of efficient and reliable IR optical sources with a silicon on insulator (SOI) platform represents a key step for the development of future telecommunications systems. For silicon photonics, III-V lasers must be efficiently coupled with the SOI-based photonic integrated circuitry (PIC): the most promising approach is to use low-temperature selective wafer bonding techniques [1]. This approach offers the possibility of exploiting two different highly optimized fabrication processes to separately manufacture the optical source and the optical signal processing/conditioning part of the PIC.

The III-V sources employed by this technology are usually based on quaternary AlInGaAs alloys grown on InP substrates [2]. The reliability of arsenide-based lasers has been largely investigated during early nineties, however, at the time the research efforts were mostly directed towards the investigation on the efficiency limitations and the sudden device failures related to the presence of extended defects. As a result, the role of gradual degradation processes on the reliability of modern heterogeneous IR sources still has to be studied in detail.

The goal of this paper is to study the gradual degradation of AlInGaAs-based laser diodes (heterogeneously integrated on a SOI platform) for applications in silicon photonics. To this aim, we performed a series of constant-current stress tests on selected devices. The experimental results indicate the presence of multiple epitaxy-related degradation mechanisms, affecting both the electrical and the optical characteristics of the devices. The correlation between those degradation phenomena highlights the role of the gradual propagation and/or generation of defects in the decrease of optical performance of the device.

2. Experimental details

In this work, we analyzed experimental III-V/Silicon IR laser diodes based on a graded index separate confinement heterostructure (GRINSCH) approach (Fig. 1a). The InAlGaAs active region (2040 μm long) is designed for an emission wavelength of 1.55 μm. In such devices, the optical mode extends from the semiconductor volume underneath the current channel (which serves as gain medium) to the dielectric waveguide directly coupled to it. The semi-transparent output mirror is a dielectric loop-mirror [3], whose reflectivity was selected through proper design of the coupling length between the two branches of the waveguide (as visible in Fig. 1b). The devices are capable of emitting up to 25 mW at 600 mA (T_{AMB} = 20 °C) and feature a typical thermal resistance $R_{TH} \approx 12$ K/W. Further details on the specific epitaxial structure of the LDs under analysis are reported in Table 1.

Devices belonging to different semiconductor dices were stressed and characterized at a fixed temperature of 45 °C by means of Keysight B2912A source-meter. A four-wire connection scheme ensured an

* Corresponding author.
E-mail address: matteo.buffolo@dei.unipd.it (M. Buffolo).

https://doi.org/10.1016/j.microrel.2018.06.058
Received 31 May 2018; Received in revised form 20 June 2018; Accepted 25 June 2018

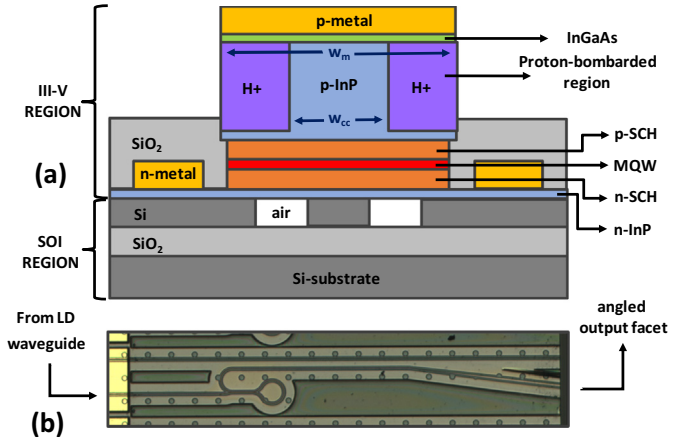

Fig. 1. (a) Schematic cross-section of the heterogeneous laser diode under investigation. Mesa and current-channel widths are respectively equal to W_m = 26 μm and W_{CC} = 4 μm (b) Detailed micrography of the dielectric semi-transparent loop-mirror integrated in the SOI region of the device.

Table 1
Detailed epitaxial structure of the III-V semiconductor region highlighted in Fig. 1. The growth direction follows the layer sequence showed in the table, from the p-contact to the n-contact.

Layer	Material	Doping (cm^{-3})	Thickness (nm)
P-contact	$In_{0.53}Ga_{0.57}As$	N_A: $2{\cdot}10^{18}$	200
Cladding	InP	N_A: $0.5–1.5{\cdot}10^{17}$	1500
P-SCH	$In_{0.53}Al_xGa_{0.47-x}As$ (x: 0.34 to 0.155)	u.i.d.	100
Barrier	$In_{0.44}Al_{0.085}Ga_{0.47}As$	u.i.d.	(8×) 9
QW	$In_{0.67}Al_{0.06}Ga_{0.26}As$	u.i.d.	(7×) 6
N-SCH	$In_{0.53}Al_xGa_{0.47-x}As$ (x: 0.155 to 0.34)	u.i.d.	100
N-contact	InP	N_D: 10^{18}	110
Superlattice	$InP/In_{0.85}Ga_{0.15}As_{0.33}P_{0.67}$	N_D: 10^{18}	(2×) 5.6/(2×) 7.5
N-InP	InP	N_D: 10^{18}	10

accurate reading of device voltage. Finally, the optical output of the LD was collected by means of an amplified germanium photodiode placed in front of the angled facet of the device, in correspondence of the semi-transparent dielectric mirror.

3. Experimental results

3.1. Thermal characterization

The thermally insulating dielectric layer of the SOI substrate represents a limiting factor for efficient high-temperature, high-current operation of heterogeneous narrow-gap optoelectronic devices. For this reason, it is important to evaluate the characteristic temperature (T_0) of the devices before stress. By fitting the I_{th}-T relation, obtained from the L-I-T measurements reported in Fig. 2, with the phenomenological relation given by

$$I_{th}(T) = I_0 e^{T/T_0}$$

we found a typical value for T_0 equal to 46.6 °C. Despite this value is quite low compared to the 100 + °C of a more traditional laser source, it falls within the range of typical characteristic temperature for heterogeneous laser sources found in literature [4, 5].

3.2. Degradation processes induced by DC aging

By submitting a series of devices with different mirror reflectivity and waveguide coupling widths to DC aging at 650 mA – T_{AMB} = 45 °C,

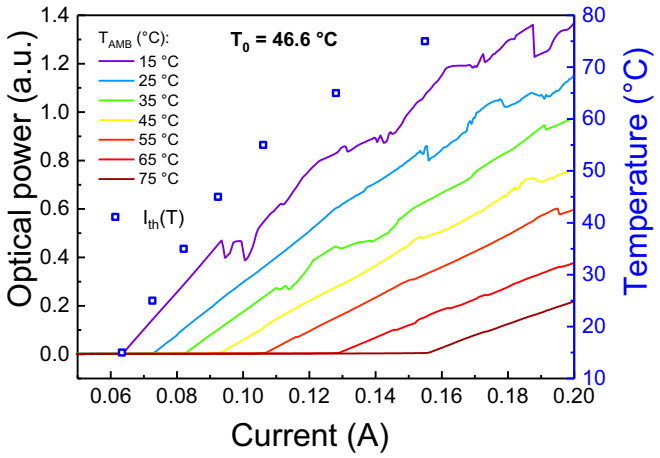

Fig. 2. L-I-T characterization of an untreated loop-mirror laser. The temperature dependence of threshold current is highlighted by the blue scatter plot.

corresponding to an approximate junction temperature of about 58.7 °C, we were able to identify a common set of degradation mechanisms, affecting both the optical and the electrical characteristics of the devices. In particular, stress was found to induce a significant increase in the threshold current of the lasers, as well as a decrease in their subthreshold emission (Fig. 3). The correlation between those two parameters, visible in the second plot of Fig. 3, suggested that the reduction in the optical performance of the device could be ascribed to the decrease in the non-radiative carrier lifetime. This hypothesis was further testified by the trend over stress time of the (relative) subthreshold emission, reported in Fig. 4. Below threshold, the spontaneous LED-like emission process dominates over stimulated emission. In particular, at very-low injection currents the optical emission is highly dependent on the balance between radiative and non-radiative recombination processes.

Since in this bias regime the latter are typically dominated by SRH recombination, a higher decrease in the spontaneous emission at lower currents with respect to higher current levels can be usually ascribed to the increase in the SRH recombination rate, as a consequence of an increase in the concentration of defects within the active region of the device [6].

With regard to their electrical characteristics, the devices exhibited a consistent decrease in the operating voltage (Fig. 5). This kind of degradation is compatible with both an annealing of the ohmic contacts, or to a change in the defect-related current components [7]. The strong correlation between the threshold current increase (related to non-radiative defects) and the decrease in the operating voltage for driving currents higher than 100 μA supports the latter hypothesis (Fig. 6), further confirming what previously observed from the trend of the optical characteristics.

The aforementioned correlation is partially lost if operating voltages at driving currents lower than 100 μA are considered. Within this bias regime, an apparent slow-down of the degradation process occurs around 100 min of stress (black line in Fig. 7).

Interestingly, this slow-down was found to be well correlated with the variation in the trend of the sub-threshold emission at very-low measuring currents (blue line in Fig. 7). In addition to that, from 30 min to 500 min of stress the device experienced a measurable 4% drop in slope efficiency, which may testify a reduction in the injection efficiency [8]. The absence of correlation between this minor variation in SE and the decrease in sub-threshold emission, i.e. the increase in defect-related recombination, can be explained by considering that above threshold all the defect-related recombination paths are saturated. Once this saturation occurs, the excess concentration of injected carriers tends to be consumed by other recombination/escape processes rather than by SRH recombination. If the stress-induced defects are not

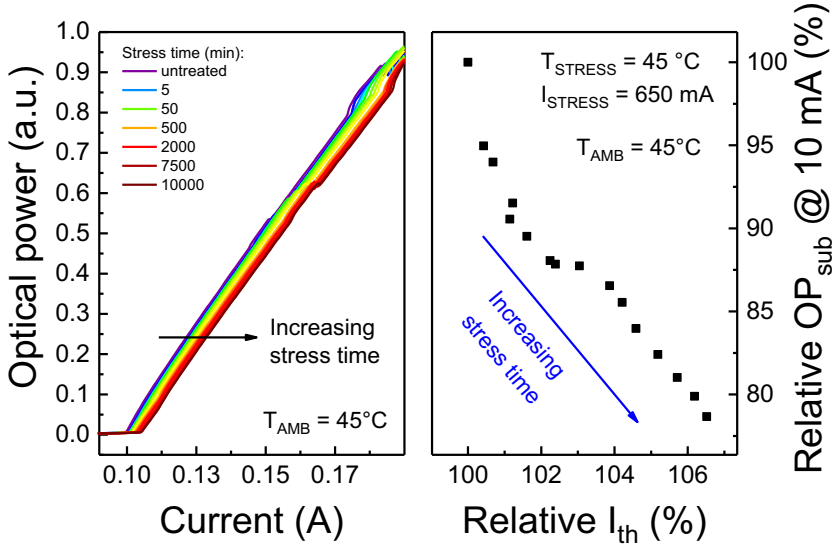

Fig. 3. L-I curves measured during DC stress at 650 mA, 45 °C. On the right: correlation between the threshold current increase and the sub-threshold emission decrease.

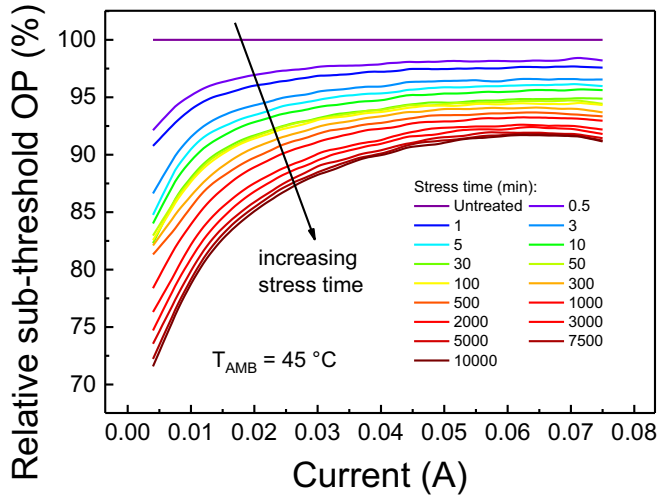

Fig. 4. Relative variation of the sub-threshold L-I curves measured at 45 °C during DC stress.

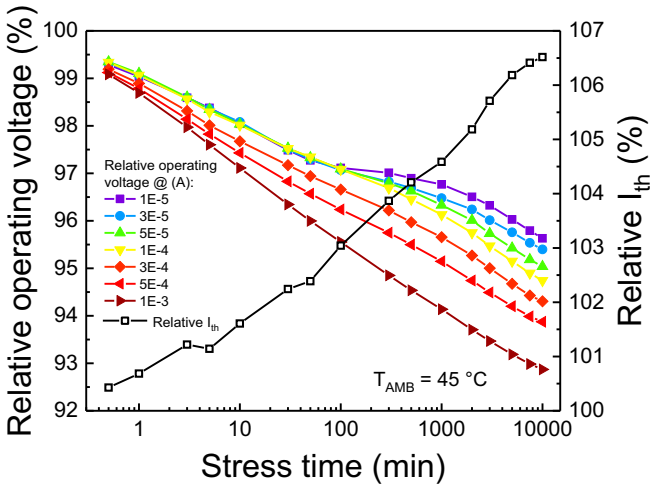

Fig. 6. Trend during stress time of the relative threshold current and of the relative operating voltages at specific drive currents.

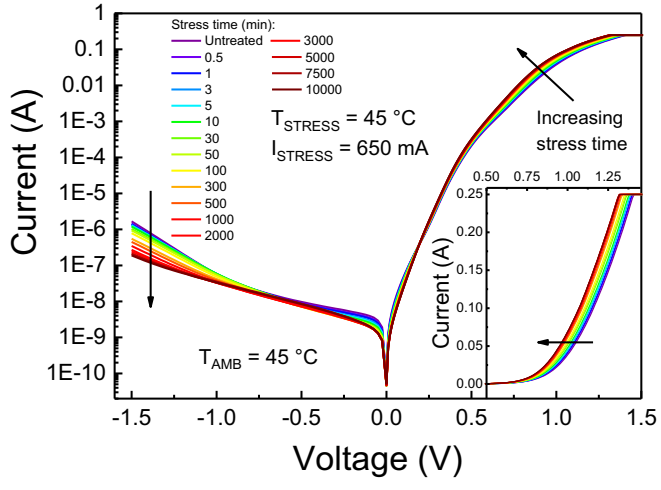

Fig. 5. I-V characteristics in linear (inset) and semi-log scales measured after each stress cycle at an ambient temperature of 45 °C.

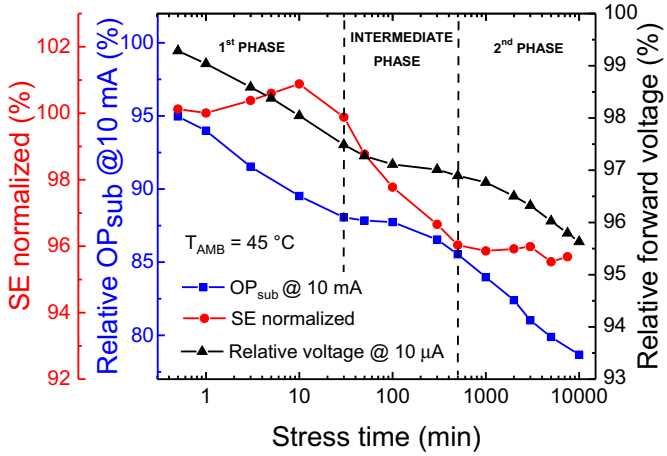

Fig. 7. Trend during stress time of the relative sub-threshold emission at 10 mA, of the relative slope-efficiency and of the relative voltage variation at 10 µA.

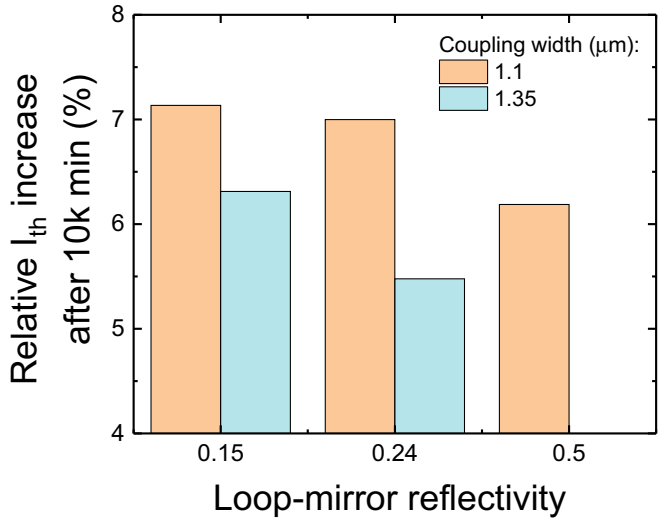

Fig. 8. Relative threshold-current variation measured after 10 k min of stress, at 650 mA and T_{AMB} = 45 °C, on five different loop-mirror laser featuring different mirror reflectivity and coupling widths with the Silicon waveguide. The sample analyzed in Section 3 features R = 0.15 and w_{Si} = 1.35.

optically-active, which would increase the internal losses of the material due to absorption, this translates into a relatively stable differential quantum efficiency at high current regimes, as described by the almost parallel shift of the L-I curves in Fig. 3.

Previous reports [9] showed that heterogeneous lasers based on the same epitaxial structure, and aged in similar conditions, experience a stress-induced relocation of free-charge (and defects) towards the active layer. Taking this into account, and considering that no new optical-cavity related degradation processes were found to affect the samples investigated in this work, our experimental data can be interpreted by identifying two distinct phases in the degradation process. During both phases the reduction in optical performance of the LD is mainly driven by the increase in SRH recombination within the active region, due the propagation/generation of defects that act as non-radiative recombination centers. As the first phase ends, after about 30–100 min of stress, the device starts experiencing a loss in injection efficiency due to the excessive accumulation of free-charge close to the active layer. The decreased injection efficiency induces an increase of the equivalent impedance offered by the device, as testified by the peculiar trend of the operating voltage (at low current levels) reported in Fig. 7. After that intermediate phase, the defect-related optical degradation of the device continues, eventually leading to a 6.5% increase in the threshold current of the device. These results confirm the conclusions on the degradation of the III-V epitaxy made in our previous work and further prove the role of defects in the optical degradation of this novel family of semiconductor devices.

3.3. Impact of cavity geometry on optical degradation

Accelerated aging at the formerly cited stress conditions, I = 650 mA and T_{AMB} = 45 °C, was carried out on four more devices, differing from the previously analyzed sample in terms of mirror reflectivity (R) and/or coupling width with the Silicon waveguide (w_{Si}). The experimental results indicated that the different cavity geometries did not impact on the degradation modes affecting the devices, whereas a significant difference in the relative amount of threshold-current increase was observed, as reported in Fig. 8.

In particular, a decreasing amount of optical degradation was found to take place on devices with increased mirror reflectivity and/or coupling width. The variation in both parameters involves the variation in optical field distribution and intensity within the optical cavity. However, due to the heterogeneous nature of the devices under investigation, the optical field is only partially interacting with the III-V active region, where stimulated emission and other optically-induced absorption and degradation mechanisms may take place. For this reason, also considering the reduced population of experimental devices analyzed so far, a more in depth investigation is needed in order to identify the physical processes responsible for the observed dependency of optical degradation.

4. Conclusions

In conclusion, with this work we investigated on the gradual degradation processes that may impact on the long-term reliability of heterogeneous III-V/Silicon IR sources for integrated telecommunication applications. A series of constant-current accelerated life tests revealed the presence of different degradation processes, affecting both the optical and the electrical characteristics of the device. The correlation between the threshold-current increase and the decrease in sub-threshold emission highlighted the role of defects in the optical degradation of the devices. Moreover, the peculiar correlation between the beginning of the second phase of optical degradation and the variation in the electrical characteristics showed that charge accumulation in proximity of the active layer of the device can lead to a slight decrease in the injection efficiency. Finally, a consistent dependence of the total amount of optical degradation on the cavity geometry was found, indicating that a trade-off between optical performance and long-term reliability exists for this novel family of optical sources.

References

[1] H. Park, M.N. Sysak, H.W. Chen, A.W. Fang, D. Liang, L. Liao, B.R. Koch, J. Bovington, Y. Tang, K. Wong, M. Jacob-Mitos, R. Jones, J.E. Bowers, Device and integration technology for silicon photonic transmitters, IEEE J. Sel. Top. Quantum Electron. 17 (2011) 671–688, http://dx.doi.org/10.1109/JSTQE.2011.2106112.
[2] M. Allovon, M. Quillec, Interest in AlGaInAs on InP for optoelectronic applications, IEE Proc. J. Optoelectron. 139 (1992) 148–152, http://dx.doi.org/10.1049/ip-j.1992.0026.
[3] Y. Zhang, S. Yang, A.E.J. Lim, G.Q. Lo, T. Baehr-Jones, M. Hochberg, Sagnac loop mirror based laser cavity for silicon-on-insulator, 2014 IEEE Opt. Interconnects Conf. OI 2014, IEEE, 2014, pp. 77–78, , http://dx.doi.org/10.1109/OIC.2014.6886087.
[4] A.W. Fang, H. Park, O. Cohen, R. Jones, M.J. Paniccia, J.E. Bowers, Electrically pumped hybrid AlGaInAs-silicon evanescent laser, Opt. Express 14 (2006) 9203, http://dx.doi.org/10.1364/OE.14.009203.
[5] H.-H. Chang, A.W. Fang, M.N. Sysak, H. Park, R. Jones, O. Cohen, O. Raday, M.J. Paniccia, J.E. Bowers, 1310 nm silicon evanescent laser, Opt. Express 15 (2007) 11466, , http://dx.doi.org/10.1364/OE.15.011466.
[6] M. Meneghini, L.-R. Trevisanello, G. Meneghesso, E. Zanoni, A review on the reliability of GaN-based LEDs, IEEE, Trans. Device Mater. Reliab. 8 (2008) 323–331, http://dx.doi.org/10.1109/TDMR.2008.921527.
[7] M. Fukuda, G. Iwane, Degradation of active region in InGaAsP/InP buried heterostructure lasers, J. Appl. Phys. 58 (1985) 2932–2936, http://dx.doi.org/10.1063/1.336298.
[8] U. Strauss, T. Lermer, J. Müller, T. Hager, G. Brüderl, A. Avramescu, A. Lell, C. Eichler, Study of defects and lifetime of green InGaN laser diodes, Phys. Status Solidi (a) 209 (2012) 481–486, http://dx.doi.org/10.1002/pssa.201100454.
[9] M. Buffolo, M. Meneghini, C. De Santi, M.L. Davenport, J.E. Bowers, G. Meneghesso, E. Zanoni, Degradation mechanisms of heterogeneous III-V/silicon 1.55-μm DBR laser diodes, IEEE J. Quantum Electron. 53 (2017) 1–8, http://dx.doi.org/10.1109/JQE.2017.2714582.